

# Unconventional spin glass behavior in the cubic pyrochlore $\text{Mn}_2\text{Sb}_2\text{O}_7$

H D Zhou<sup>1,2</sup>, C R Wiebe<sup>1,2</sup>, A Harter<sup>2,3</sup>, N S Dalal<sup>2,3</sup> and J S Gardner<sup>4,5</sup>

<sup>1</sup> Department of Physics, Florida State University, Tallahassee, FL 32306-3016, USA

<sup>2</sup> National High Magnetic Field Laboratory, Florida State University, Tallahassee, FL 32306-4005, USA

<sup>3</sup> Department of Chemistry, Florida State University, Tallahassee, FL 32306-4390, USA

<sup>4</sup> NIST Center for Neutron Research, Gaithersburg, MD 20899-6102, USA

<sup>5</sup> Indiana University, 2401 Milo B Sampson Lane, Bloomington, IN 47408, USA

E-mail: [cwiebe@magnet.fsu.edu](mailto:cwiebe@magnet.fsu.edu)

Received 5 May 2008, in final form 20 June 2008

Published 9 July 2008

Online at [stacks.iop.org/JPhysCM/20/325201](http://stacks.iop.org/JPhysCM/20/325201)

## Abstract

The new pyrochlore  $\text{Mn}_2\text{Sb}_2\text{O}_7$  has been synthesized via a low-temperature method to retain cubic  $Fd\bar{3}m$  symmetry. The resulting material has an unconventional spin glass state at  $T_{\text{SG}} \sim 41$  K, in the absence of detectable site disorder or a structural phase transition. A peak in the DC susceptibility at  $T_{\text{SG}}$ , and a characteristic shift in the real part of the AC susceptibility was noted, but with a slightly more dynamic state than predicted through the typical Mydosh spin glass parameter of  $\Delta T_{\text{SG}}/[T_{\text{SG}} \log(\omega)]$ . Time-dependent magnetization measurements show glassy behavior below 41 K. Elastic neutron scattering measurements on powder samples show significant magnetic diffuse scattering from the Mn spins beneath the transition, similar to the scattering observed in the spin liquid  $\text{Tb}_2\text{Ti}_2\text{O}_7$ . The dynamic character of  $\text{Mn}_2\text{Sb}_2\text{O}_7$  is inferred to arise from the frustration inherent within the pyrochlore lattice.

Materials experiencing geometric frustration (GF) have been a topic of much recent interest. The pyrochlores in particular, of general chemical formula  $\text{A}_2\text{B}_2\text{O}_7$ , have dominated much of the literature due to the plethora of interesting ground states without long magnetic range order, such as spin glasses, spin ices, and spin liquids [1]. In conventional spin glasses, randomness and frustration are both essential. But for some pyrochlores, such as  $\text{Y}_2\text{Mo}_2\text{O}_7$ ,  $\text{Tb}_2\text{Mo}_2\text{O}_7$ , and  $\text{Y}_2\text{Mn}_2\text{O}_7$  [2–4], spin glass ordering is observed without apparent chemical disorder. These unusual phase transitions have atypical critical exponents, and the ground states are ill-defined both experimentally and theoretically [5].

The pyrochlore series  $\text{A}_2\text{Sb}_2\text{O}_7$  (A = transition metal ion) represents a new arena for the search for exotic ground states. Most of the studied pyrochlores have magnetic ions on the B site with six-fold oxygen coordination.  $\text{Mn}_2\text{Sb}_2\text{O}_7$  is a potential pyrochlore with magnetic  $\text{Mn}^{2+}$  ions on the A sites with eight-fold oxygen coordination. Scott prepared  $\text{Mn}_2\text{Sb}_2\text{O}_7$  by the solid state reaction of  $\text{MnCO}_3$  and  $\text{Sb}_2\text{O}_3$  at 1373 K, and reported that its crystal structure is trigonal  $P3_121$  which is fluorite-related, but not a distorted pyrochlore [6].

Furthermore, Reimers *et al* reported there is a long range magnetic ordering in this distorted sample [7]. Until now no physical properties have been reported on  $\text{Mn}_2\text{Sb}_2\text{O}_7$  with the cubic pyrochlore structure. Here we report a low-temperature method to synthesize the cubic  $\text{Mn}_2\text{Sb}_2\text{O}_7$ . The magnetic properties of this new sample exhibit an unusual spin glass transition at  $T_{\text{SG}} = 41$  K.

A polycrystalline sample of  $\text{Mn}_2\text{Sb}_2\text{O}_7$  was made through a low-temperature solid state reaction. Mixtures of acetate  $\text{Mn}(\text{Ac})_2 \cdot \text{H}_2\text{O}$  and antimonic acid  $\text{Sb}_2\text{O}_5 \cdot x\text{H}_2\text{O}$  in the appropriate ratios were ground together and calcined in air at 423 K for 12 h, then reground and finally calcined in air at 723 K for 12 h. The x-ray powder diffraction (XRD) patterns were recorded with a Guinier image plate with  $\text{Cu K}\alpha_1$  radiation (1.54059 Å) and a Ge monochromator. Data were collected in steps of  $0.005^\circ$  over the range  $26^\circ \leq 2\theta \leq 100^\circ$  with temperatures down to 10 K obtained with a He compressor. XRD data was fit from the Rietveld refinement by using program FullProf with typical  $R_p \approx 6.0$ ,  $R_{\text{wp}} \approx 6.0$  and  $\chi^2 \approx 3.0$ . AC and DC magnetic susceptibility measurements were made in a liquid helium cryostat at temperatures down

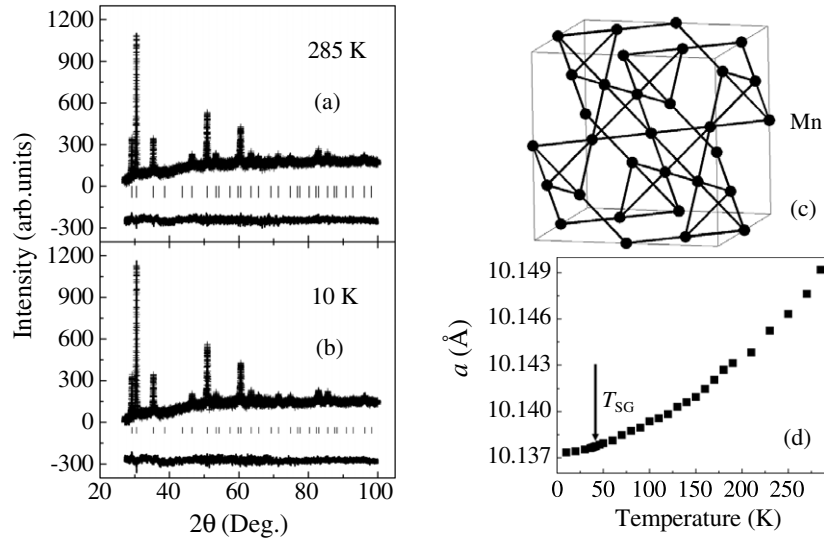


**Figure 1.** XRD patterns for  $\text{Mn}_2\text{Sb}_2\text{O}_7$  at (a) 285 K and (b) 10 K. The solid curves are the best fits from the Rietveld refinement using FullProf. The vertical marks indicate the position of Bragg peaks, and the bottom curves show the difference between the observed and calculated intensities. (c) The corner-shared lattice topology of Mn spins in  $\text{Mn}_2\text{Sb}_2\text{O}_7$ . (d) Temperature dependence of the lattice parameter.

**Table 1.** Room temperature crystallographic parameters and selected bond lengths for  $\text{Mn}_2\text{Sb}_2\text{O}_7$  ( $a = 10.1491(1)$  Å).

Atom	$x$	$y$	$z$	$B$ (Å <sup>2</sup> )
Mn	0.5	0.5	0.5	2.50(4)
Sb	0.0	0.0	0.0	1.50(7)
O(1)	0.3345(2)	0.125	0.125	2.30(7)
O(2)	0.375	0.375	0.375	2.40(7)
Mn–O(1)	2.4199(2) (Å)			
Mn–O(2)	2.1974(2) (Å)			
Sb–O(1)	2.0133(3)(Å)			

to 1.8 K. Neutron diffraction measurements were completed at NIST using the BT-1 spectrometer with a wavelength of 1.54 Å.

Room temperature XRD shows that  $\text{Mn}_2\text{Sb}_2\text{O}_7$  has a  $Fd\bar{3}m$  cubic structure with  $a = 10.1491(1)$  Å. The Rietveld refinement shows that the magnetic  $\text{Mn}^{2+}$  ions occupy the A sites and the non-magnetic  $\text{Sb}^{5+}$  ions occupy the B sites. A bond valence sum calculation has been performed based on the structural data in table 1. The results show that the Mn valence is +1.8(2) and the Sb valence is +4.9(2), which further confirms the existence of magnetic  $\text{Mn}^{2+}$  and non-magnetic  $\text{Sb}^{5+}$  ions.

The Curie–Weiss fitting of the high-temperature susceptibility data (figure 2(a)) gives a Curie–Weiss constant  $\theta = -43$  K and  $\mu_{\text{eff}} = 5.2 \mu_{\text{B}}$ . This  $\mu_{\text{eff}}$  is slightly smaller than that typically found for  $\text{Mn}^{2+}$  ( $\mu_{\text{eff}} = 5.9 \mu_{\text{B}}$ ), which is common for magnetically frustrated systems. The inset of figure 2(a) shows the temperature dependences of both zero field cooled (ZFC) and field cooled (FC) DC susceptibility measured at  $\mu_0 H = 0.1$  T. The ZFC branch presents a pronounced peak at  $T_{\text{SG}} = 41$  K, below which the ZFC and FC curves separate. This behavior is similar to the spin glass transition in  $\text{Y}_2\text{Mo}_2\text{O}_7$  [2]. We speculate that the transition observed here is also a spin glass transition. The magnetization measured as

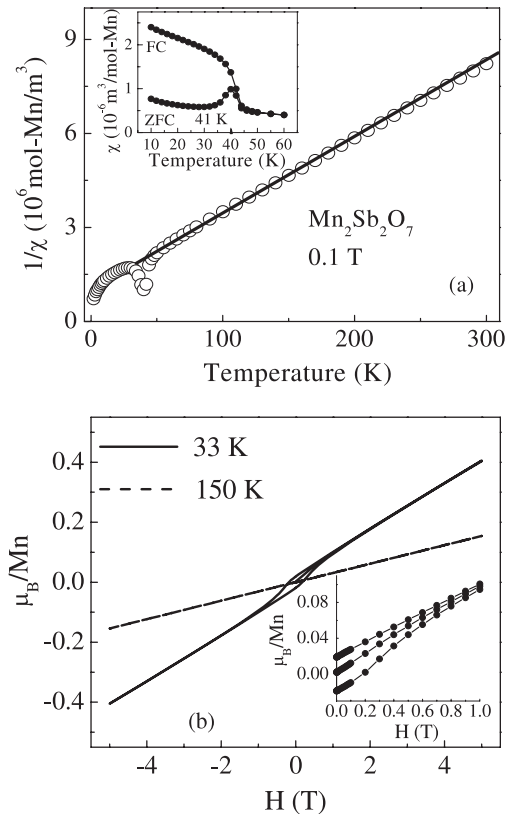


**Figure 2.** (a) Temperature dependence of the inverse of DC susceptibility; open circles are experimental data and the line is the Curie–Weiss fitting. Inset: susceptibility around 40 K. (b)  $M$ – $H$  curves at 33 and 150 K. Inset: low field portion of the  $M$ – $H$  curve at 33 K.

a function of field,  $M(H)$  (figure 2(b)), does not saturate even at the highest field of 5 T, which is consistent with the expected behavior of a spin glass.

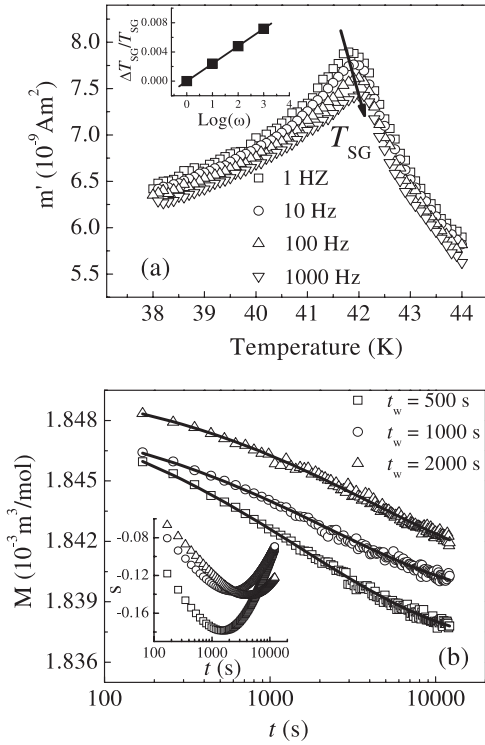


**Figure 3.** (a) Temperature dependence of the real component of the AC magnetization,  $m'$ , for  $\text{Mn}_2\text{Sb}_2\text{O}_7$  with different frequencies ( $\omega$ ). Inset: the variation of  $\Delta T_{\text{SG}}/T_{\text{SG}}$  with  $\log[\omega]$ . (b) Thermoremanent magnetization (TRM) relaxation for  $\text{Mn}_2\text{Sb}_2\text{O}_7$  with different waiting time ( $t_w$ ). Open symbols are experimental data and the solid lines are the fits of equation (1). Inset: relaxation rate  $S(t)$  for the measurements presented in the main panel.

In the case of a spin glass, the real component of the AC magnetization should exhibit a sharp and frequency-dependent cusp. The position of the cusp defines the freezing temperature  $T_{\text{SG}}$ . Figure 3(a) shows the real part ( $m'$ ) of the AC magnetization of  $\text{Mn}_2\text{Sb}_2\text{O}_7$  measured at  $\mu_0 H_{\text{dc}} = 0.0005$  T. The real part  $m'$  shows a peak at  $T_{\text{SG}} = 41$  K. The peak shifts to lower temperatures and its intensity increases as the frequency of the excitation field decreases. This behavior is a typical feature of the dynamics of spin glass systems. A quantitative measure of the frequency shift is obtained from the Mydosh parameter  $\phi \Delta T_{\text{SG}}/[T_{\text{SG}} \log(\omega)]$ . The estimated  $\Delta T_{\text{SG}}/[T_{\text{SG}} \log(\omega)] = 0.002(5)$  is near the expected range of 0.004–0.018 for conventional spin glass systems [8], although slightly more dynamic than conventional spin glasses.

The existence of spin glass behavior has also been explored through the time-dependent magnetization measurements. In this case, thermoremanent magnetization (TRM) experiments were performed. The TRM procedure in this work was the following: the sample was field cooled ( $\mu_0 H = 0.03$  T) down from 300 to 33 K; after temperature stabilization for a certain time ( $t_w$ ), the field was reduced to zero and the magnetization was recorded as a function of the elapsed time. The results for different values of  $t_w$  (500, 1000, and 2000 s) are shown in figure 3(b). All the curves can be described by the stretched exponential model,

$$M(t) = M_0 + M_r \exp[-(t/t_p)^{1-n}] \quad (1)$$

here  $M_0$  relates to an intrinsic ferromagnetic component and  $M_r$  to a glassy component mainly contributing to the relaxation observed effects. Both  $M_r$  and  $t_p$  (the time constant) depend on temperature ( $T$ ) and  $t_w$ , while  $n$  is only a function of  $T$ . If  $n = 0$ , there is a single time constant, exponential relaxation; and if  $n = 1$ , there is no relaxation at all. The solid curves in figure 3(b) are the best fits of equation (1) to the experimental data, with parameters  $1.837 < M_0 < 1.840 \times 10^{-3} \text{ m}^3 \text{ mol}^{-1}$ ,  $0.010 < M_r < 0.013 \times 10^{-3} \text{ m}^3 \text{ mol}^{-1}$ , and  $n = 0.5$  (fixed through all of the fittings). The single parameter which shows a large variation with changes in the wait time is the time constant  $t_p$ , which goes from  $t_p = 1536$  s for  $t_w = 500$  s to  $t_p = 2200$  s for  $t_w = 1000$  s, and to  $t_p = 4220$  s for  $t_w = 2000$  s. The changes observed in  $M(t)$  measured for different values of  $t_w$  demonstrate the occurrence of aging effects. In the inset of figure 3(b) this point is emphasized by showing the relaxation rate  $S(t) = dM/d \ln(t)$ . The shift of the minimum position of  $S(t)$  is clearly observed, which is expected to occur for a spin glass system.

The DC and AC magnetization data all support spin glass behavior in  $\text{Mn}_2\text{Sb}_2\text{O}_7$ . However, there are several open questions: How can a disorder-free system give rise to spin glass behavior? What spatial correlations are associated with this transition? Neutron scattering experiments have been performed to directly address this problem. The neutron diffraction pattern taken at 4 and 80 K (figure 4) show several features: (i) no magnetic Bragg peaks or intensity changes are visible at 4 K. This result confirms that there is no structural distortion below  $T_{\text{SG}}$  and the transition at  $T_{\text{SG}}$  is not a long range magnetic ordering. (ii) By subtracting the 80 K data as a background from the 4 K data, the net scattering shows a diffuse signal which peaks near  $Q_{\text{max}} = 1.2$  and  $2.7 \text{ \AA}^{-1}$  (figure 4(b)). This magnetic contribution is consistent with an expression used to model the scattering from powders where short range, isotropic spin correlations exist out to the first few coordination shells of neighbors. This expression [9] is

$$I(Q) \sim \sum_{i,j} \langle S_i S_j \rangle \frac{\sin(Qr_{i,j})}{(Qr_{i,j})}, \quad (2)$$

which simplifies to

$$I(Q) \sim \frac{\sin(QR)}{(QR)} \quad (3)$$

if the spins are correlated over nearest neighbors, and consequently only one value  $R$  of  $r_{i,j}$  (the distance between spins at site  $i$  and  $j$ ) is employed. This expression multiplied by the magnetic form factor of the  $\text{Mn}^{2+}$  ion has been fit to the net intensity shown in figure 4(b). The fit gives a  $R = 4.1 \text{ \AA}$ , which is close to the nearest neighbor distance,  $3.7 \text{ \AA}$ , between the  $\text{Mn}^{2+}$  ions. This result indicates that whatever spin correlations are present, they must be of very short range over near neighbors only. Also note how the function has a negative value at  $Q = 0$ , indicative of antiferromagnetic correlations  $\langle S_i S_j \rangle$ . In another pyrochlore spin glass  $\text{Y}_2\text{Mo}_2\text{O}_7$  with  $T_{\text{SG}} = 22.5$  K [5], the diffuse scattering shows a peak at  $Q_{\text{max}} = 0.44 \text{ \AA}^{-1}$  and the extracted correlation length is around  $5 \text{ \AA}$ , which indicates that the short range spin correlations

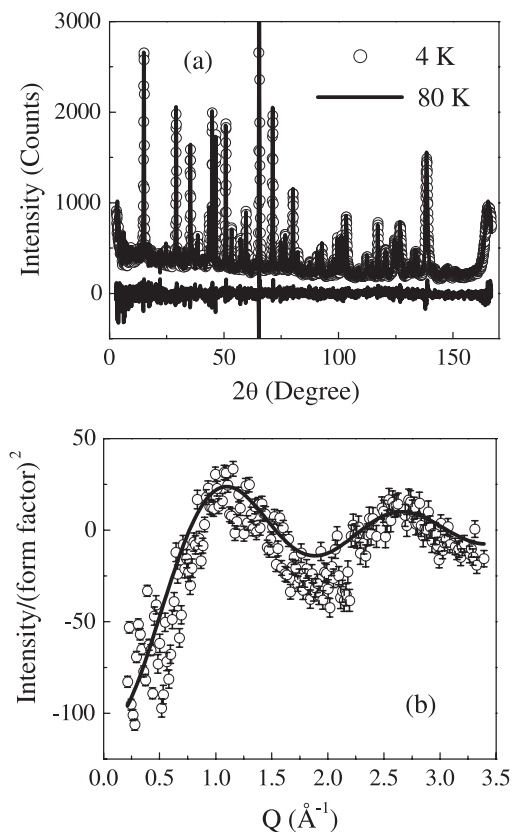


**Figure 4.** (a) Neutron diffraction measurements for  $\text{Mn}_2\text{Sb}_2\text{O}_7$  at different temperatures; circles are 4 K data and the line is 80 K data. The bottom curve shows the difference between them. (b) The difference between patterns taken at 4 and 80 K at low  $Q$ ; the circles are experimental data and the solid line is the fit to equation (3).

extend over a single conventional cell [2]. By comparison, in the cooperative paramagnetic pyrochlore  $\text{Tb}_2\text{Ti}_2\text{O}_7$ , the diffuse scattering peaks at  $Q_{\text{max}} = 1.2$  and  $3 \text{ \AA}^{-1}$ , which shows that Tb spins are correlated over only a single tetrahedron [10]. Therefore, the spin–spin correlations in  $\text{Mn}_2\text{Sb}_2\text{O}_7$  appear to be more like the spin liquid ( $\text{Tb}_2\text{Ti}_2\text{O}_7$ ) rather than the spin glass ( $\text{Y}_2\text{Mo}_2\text{O}_7$ ) pyrochlores, and this could be the explanation for the small  $\Delta T_{\text{SG}}/[T_{\text{SG}} \log(\omega)]$  value seen in the analysis of the magnetic susceptibility. However, high energy resolution neutron scattering experiments are needed to truly understand the spin dynamics in this system.

What drives this spin glass transition? It appears that the degree of chemical disorder is very low. The best refinement of the room temperature XRD pattern is obtained with  $\text{Mn}^{2+}$  on the A site and  $\text{Sb}^{5+}$  on the B site. The XRD data shows there is no chemical disorder down to the few percentage level. Several other simple arguments also support the chemical ordering of Mn and Sb ions in the structure: (i) the large charge difference between  $\text{Mn}^{2+}$  ( $3d^5$ ) and  $\text{Sb}^{5+}$  ( $4d^{10}$ ); (ii) the large ionic size difference between  $\text{Mn}^{2+}$  ( $r^{\text{VIII}} = 0.96 \text{ \AA}$ ) and  $\text{Sb}^{5+}$  ( $r^{\text{VI}} = 0.60 \text{ \AA}$ ); (iii)  $\text{Mn}^{2+}$  prefers an eight-fold coordination site and  $\text{Sb}^{5+}$  prefers a six-fold coordination site [11]. Without apparent chemical disorder in the sample, could there be a structural distortion to induce this transition? The neutron data shown above suggests that there is no structural phase

transition down to 4 K. As shown in figure 1, XRD at 10 K shows the sample still retains cubic symmetry, and the temperature dependence of the lattice parameter shows no anomaly at  $T_{\text{SG}}$ .

The glassiness of the system implies some kind of disorder in the exchange integral, whose origin might be a deformation in the local ionic environment. Indeed, Booth *et al* showed, using the x-ray absorption fine structure (XAFS) technique, that the Mo tetrahedra of  $\text{Y}_2\text{Mo}_2\text{O}_7$  are in fact distorted at the local level by roughly 5% [12]. This amount of bond disorder is not seen by the usual diffraction techniques (x rays or neutrons), indicating that the average bulk structure is almost the perfect oxide pyrochlore lattice [13]. Further evidence for this disorder of  $\text{Y}_2\text{Mo}_2\text{O}_7$  was revealed by  $^{89}\text{Y}$  NMR [14] and  $\mu\text{SR}$  [15] results. A recent theoretical calculation has verified that extremely weak disorder can induce spin freezing in geometrically frustrated antiferromagnets [16]. Here the glassiness of  $\text{Mn}_2\text{Sb}_2\text{O}_7$  could be due to the same reason—the existence of a local deformed lattice that is difficult to detect via diffraction techniques.

In conclusion, a spin glass transition is observed for the new cubic pyrochlore  $\text{Mn}_2\text{Sb}_2\text{O}_7$  with magnetic ions on the A sites. This transition occurs without apparent chemical disorder and structural distortion, which makes this material another example of a spin glass phase induced by frustration effects inherent from the pyrochlore structure. The possible reason for the glassiness could be the local deformed lattice, which needs further confirmation through XAFS, NMR, or  $\mu\text{SR}$  experiments.

## Acknowledgments

This work utilized facilities supported in part by the NSF under Agreement No. DMR-0084173. A portion of this work was made possible by the NHMFL In-House Research Program, the EIEG program, the State of Florida, and the DOE. We acknowledge useful discussions with Professor J E Greedan.

## References

- [1] Greedan J E 2001 *J. Mater. Chem.* **11** 37
- [2] Gardner J S, Lee S H, Broholm C, Raju N P and Greedan J E 1999 *Phys. Rev. Lett.* **83** 211
- [3] Gaulin B D, Reimers J N, Mason T E, Greedan J E and Tun Z 1992 *Phys. Rev. Lett.* **69** 3244
- [4] Reimers J N, Greedan J E, Kremer R K, Gmelin E and Subramanian M A 1991 *Phys. Rev. B* **43** 3387
- [5] Gingras M J P, Stager C V, Raju N P, Gaulin B D and Greedan J E 1997 *Phys. Rev. Lett.* **78** 947
- [6] Scott H G 1987 *J. Solid State Chem.* **66** 171
- [7] Reimers J N, Greedan J E, Stager C V and Bjorgvinnsen M 1991 *Phys. Rev. B* **43** 5692
- [8] Mydosh J A 1993 *Spin Glasses: An Experimental Introduction* (London: Taylor and Francis)
- [9] Bertaut E F and Burel P 1967 *Solid State Commun.* **5** 27
- [10] Gardner J S, Dunsiger S R, Gaulin B D, Gingras M J P, Greedan J E, Kiefl R F, Lumsden M D, MacFarlane W A and Raju N P 1999 *Phys. Rev. Lett.* **82** 1012
- [11] Shannon R D 1976 *Acta Crystallogr. A* **32** 751

- [12] Booth C H, Gardner J S, Kwei G H, Heffner R H, Bridges F and Subramanian M A 2000 *Phys. Rev. B* **62** [R755](#)
- [13] Raju N P, Gmelin E and Kremer R K 1992 *Phys. Rev. B* **46** [5405](#)
- [14] Keren A and Gardner J S 2001 *Phys. Rev. Lett.* **87** [177201](#)
- [15] Sagi E, Ofer O, Keren A and Gardner J S 2005 *Phys. Rev. Lett.* **94** [237202](#)
- [16] Saunders T E and Chalker J T 2007 *Phys. Rev. Lett.* **98** [157201](#)